


A comparative study of U937 cell size changes during apoptosis initiation by flow cytometry, light scattering, water assay and electronic sizing

Valentina Yurinskaya¹ · Nikolay Aksenov¹ · Alexey Moshkov¹ · Michael Model² · Tatyana Goryachaya¹ · Alexey Vereninov¹ 

Published online: 31 July 2017
© Springer Science+Business Media, LLC 2017

Abstract A decrease in flow cytometric forward light scatter (FSC) is commonly interpreted as a sign of apoptotic cell volume decrease (AVD). However, the intensity of light scattering depends not only on the cell size but also on its other characteristics, such as hydration, which may affect the scattering in the opposite way. That makes estimation of AVD by FSC problematic. Here, we aimed to clarify the relationship between light scattering, cell hydration (assayed by buoyant density) and cell size by the Coulter technique. We used human lymphoid cells U937 exposed to staurosporine, etoposide or hypertonic stress as an apoptotic model. An initial increase in FSC was found to occur in apoptotic cells treated with staurosporine and hypertonic solutions; it is accompanied by cell dehydration and is absent in apoptosis caused by etoposide that is consistent with the lack of dehydration in this case. Thus, the effect of dehydration on the scattering signal outweighs the effect of reduction in cell size. The subsequent FSC decrease, which occurred in parallel to accumulation of annexin-positive cells, was similar in apoptosis caused by all three types of inducers. We conclude that an increase, but not a decrease in light scattering, indicates the initial cell volume decrease associated with apoptotic cell dehydration.

Keywords Apoptosis · Apoptotic volume decrease · Flow cytometer light scattering · Cell water · Cell volume assay

✉ Alexey Vereninov
verenino@gmail.com

¹ Institute of Cytology, Russian Academy of Sciences, St-Petersburg, Russia

² Department of Biological Sciences, Kent State University, Kent, OH 44242, USA

Introduction

Cell shrinkage and apoptotic volume decrease (AVD) are considered an important early stage of apoptosis [1–6]. A common way to detect AVD is by forward light scattering (FSC) on a flow cytometer [7–12]. It is known, however, that light scattering depends on many factors other than cell size [13]. One of them is cell hydration. However, it is specifically cell dehydration that is thought to be a major mechanism of AVD [6, 14–17].

Comparative study of light scattering during apoptosis induced by etoposide, staurosporine (STS) and hypertonic stress is interesting because of different patterns of changes in cell hydration during initiation of apoptosis in these cases. Apoptosis induced in U937 cells by etoposide is the best example of apoptosis without an initial water loss; staurosporine provides an opposite case of apoptosis with the typical cell dehydration; hypertonic stress initiates apoptosis by direct osmotic loss of cell water [3, 14–16, 18–20]. The results presented below show flow cytometry data in parallel with cell water assay by buoyant density and Coulter cell sizing. We show that an increase, but not a decrease, in light scattering marks the initial cell volume decrease associated with apoptotic cell dehydration if the latter takes place at all. The delayed FSC decrease paralleled the accumulation of annexin-positive cells and was similar in apoptosis caused by all of the studied inducers. The popular view that a decrease in FSC accompanies the initiation of apoptosis is inconsistent with the data obtained on U937 cells. We suppose that this view took hold because cell fragments with reduced sizes were viewed as early apoptotic cells. Only whole cells identified on FSC/SSC contour plots and tested for early apoptosis by annexin and propidium iodide (PI) were analyzed in the present study.

Materials and methods

Cell culture, drug treatment and chemicals

U937 human histiocytic lymphoma cells were obtained from the Russian Cell Culture Collection (Institute of Cytology, Russian Academy of Sciences, St. Petersburg, cell line U937 catalogue number 160B2). The cells were cultured in RPMI 1640 medium (Biolot, Russia) with 10% fetal calf serum (HyClone, USA) in an atmosphere of 95% air and 5% CO₂ at 37 °C. Cells were grown to densities of 1×10^6 cells/ml before use and prepared for experiment on day 1 or 2 of culture. For induction of apoptosis, the cells were exposed to STS (Sigma-Aldrich, Germany), etoposide (Sigma-Aldrich, Germany) or hypertonic medium. Stock solutions of STS (2 mM) and etoposide (34 mM) in DMSO were used to yield the final concentrations of 1 μM STS and 50 μM etoposide. Hypertonic media were prepared by addition to RPMI medium of 180 mM sucrose or 100 mM NaCl from the stock solutions of 2 M sucrose in PBS and 1 M NaCl, respectively. The osmolarity of solutions was checked with the Micro-osmometer Model 3320 (Advanced Instruments, USA). Sucrose and NaCl were of analytical grade from Reachim (Russia). Alexa Fluor 647 Annexin V (annexin) was purchased from Life Technologies (USA) and PI was from Immunochemistry Technologies (USA). Percoll was from Pharmacia (Sweden). Density marker beads were from Sigma (Germany).

Cell size and buoyant density assay

Cell size was measured by Scepter cell counter equipped with a 40-μm sensor and software version 2.1, 2011 (Merck Millipore, Germany). After treatment with apoptosis inducers for appropriate time periods, the cells were centrifuged at 2000×g and re-suspended in Hank's balanced salt solution (HBSS) or in hypertonic HBSS with added sucrose or NaCl. At the same time, cells were diluted to concentrations of $(0.5 - 1) \times 10^6$ cells/ml, which lie within the operating range of the instrument. An increase in the conductivity of the media due to addition of 100 mM NaCl decreases the apparent particle size by about 20%, as was verified by running standard 10 μm polystyrene microparticles (Sigma-Aldrich Product No 72986). Only the corrected data are presented on the graphs.

Cell water was determined by measurements of the buoyant density of cells in continuous Percoll gradients. In our experience, this is the most sensitive and reliable of all currently existing methods for determination of cell water [14, 15, 17, 20, 21]. Density marker beads were used to calibrate density gradients. The water content per g protein, v_{prot} , was calculated as $v_{\text{prot}} = (1 - \rho/\rho_{\text{dry}})/[0.72(\rho - 1)]$, where ρ is the measured buoyant density of

the cells and ρ_{dry} is the density of the cell dry mass, the latter taken as 1.38 g/ml. The ratio of protein to dry mass was taken as 0.72. Relative changes in cell water do not depend noticeably on the assumed values of ρ_{dry} or on the ratio of protein to dry mass.

Flow cytometric analysis

The dynamics of apoptosis induced by etoposide, STS and hypertonic stress was studied by flow cytometry. Samples were analyzed on a CytoFLEX Flow Cytometer (Xitogen Technologies, Suzhou, China) equipped with three lasers (405, 488 and 638 nm) and nine detectors. The apoptosis assay utilized annexin V and PI as probes for phosphatidylserine outer leaflet exposure and non-selective membrane permeability, respectively. The annexin fluorescence was measured in the APC-A700 channel (638-nm excitation, 712/25 nm bandpass emission filter), and PI fluorescence was measured in the PE channel (488-nm excitation, 585/42 nm bandpass emission filter). For subsequent analysis with CytExpert software (Xitogen Technologies, Suzhou), at least 2×10^4 events in the "cell" area of the FSC versus SSC dot plots were collected per sample.

For staining with annexin and PI, control cells or cells after induction of apoptosis were washed with PBS and re-suspended in the annexin-binding buffer (140 mM NaCl, 2.5 mM CaCl₂, 10 mM HEPES/NaOH, pH 7.4). 5 μl of annexin and 2 μl of PI (0.25 mg/ml) were subsequently added to 100 μl of cell suspension. 180 mM sucrose or 100 mM NaCl were added during washing and cell staining, as appropriate. After 15–20 min of incubation at room temperature, cells were diluted to 500 μl with annexin-binding buffer and analyzed on a CytoFLEX Flow Cytometer. Annexin-positive, PI-negative cells were counted as early apoptotic, annexin, PI-positive cells - as dead. For analysis of annexin and PI fluorescence, cells were gated on FSC with threshold at 2×10^4 . Annexin-positive and annexin-negative cells were selected on contour plots where boundaries between cell populations are more visible.

Statistical analysis

The medians of the FSC, SSC, APC-A700-A or PE-A areas for appropriate cell subpopulations given by CytExpert 1.2.8.0 software were averaged for all samples analyzed. Using the means leads practically to the same results as using the medians. The averaged median data were expressed as Mean ± SE for indicated numbers of experiments and were analyzed using Student's *t* test. $P < 0.05$ was considered as statistically significant.

Results

Major particle subsets in the entire cell culture as revealed by the FSC/SSC contour plots

Whole cells and residual particles present in FSC/SSC contour plots form two distinct major subsets denoted below as P0 and P1 (Fig. 1). The former is rather scattered whereas the latter is compact. The gap between them is reduced as apoptosis progresses. The P0 and P1 subsets made up about 40 and 60% of the entire control cell population, respectively. The subset P0 increased significantly in cultures induced to apoptosis. The observed increase of P0 is a well-known phenomenon, which is a specific feature of apoptosis [11, 22, 23]. The kinetics of P0 particles generation in U937 cell culture treated with all tested apoptosis inducers is shown in Fig. 2. The number of P0 particles increases significantly only after 3–4 h or a little earlier in cells treated with hypertonic media ($P < 0.05$). It should be noted that some authors consider subsets similar to P0 as apoptotic cells with reduced FSC and annexin staining. Indeed, the P0 particles bound annexin. However, one can assume that cell fragments could be stained with annexin as the P1 cells. The number of cells in the P1 subsets was kept at the level 2×10^4 in all samples and used as a reference in estimation of sizes of all other subsets. Current study focuses on the analysis of initial stages of apoptosis in unfragmented P1 cells. The origin of P0 is beyond the scope of the current article.

Apoptosis progress in the cell subpopulation P1 as revealed by annexin-propidium iodide test

The cell subpopulation P1, which appears homogeneous in the FSC/SSC plots, splits into distinct groups in the annexin versus PI plots (Fig. 3a). Two major (P2, P3) and

one minor subset (P4) are distinguishable after treatment with apoptosis inducers for sufficient time (Fig. 3a). Cells with low fluorescence in both channels (P2) can be operationally classified as pre-apoptotic. Cells with strong annexin but low PI signal are classified, in agreement with current views, as early apoptotic (Fig. 3a, P3). The remaining 2–5% of P1 cells (P4) that are double annexin-PI positive represent late apoptosis (Fig. 3a, P4). The analog of the P2 subset can be seen in unstained samples (Fig. 3b). The signal in the “Annexin” channel in this case is caused by autofluorescence. It should be noted that the positions of subsets P2 in plots for stained and unstained samples do not fully coincide. This fact might be due to the ability of normal cells to be slightly stained with annexin when it is present in the medium. Remarkable increase in number of early apoptotic cells P3 occurs at 3–4 h. This corresponds to the time when the number

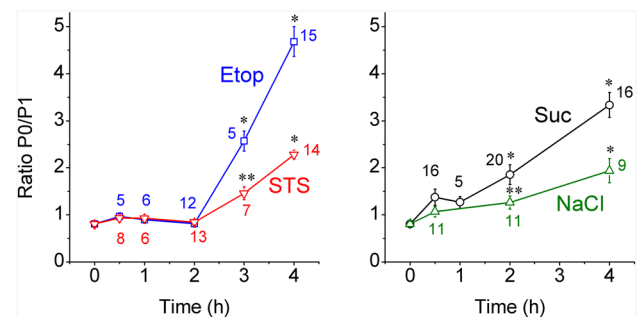


Fig. 2 The increase of size of microparticle population (P0) in U937 cell cultures after treatment with etoposide, STS and hypertonic sucrose or NaCl solutions as related to the size of populations P1 (see Fig. 1 for their selection). Means \pm SE of the ratios of P0 to P1 are shown. The number of experiments used for calculations of P0/P1 ratios for each time point is indicated on graphs. *, ** $P < 0.001$ and 0.05, respectively, as compared to untreated cells ($t = 0$). Typical experiment is shown on Fig. 1

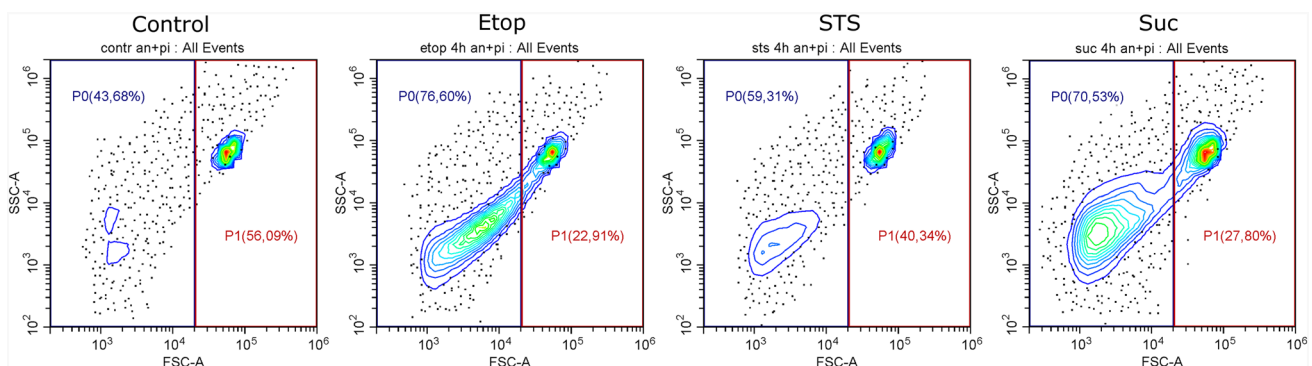


Fig. 1 FSC/SSC contour plots showing two major particle subsets, P0 and P1 in U937 cell cultures before and after 4 h treatment with etoposide (Etop), STS and hypertonic sucrose solution (Suc). All plots are results of one representative experiment in which cells

were stained with annexin and PI. The percentages of P0 and P1 were obtained after selection of two rectangular gates in CytExpert software. Percentages of gated cells in stained and not stained cell samples are similar within standard error

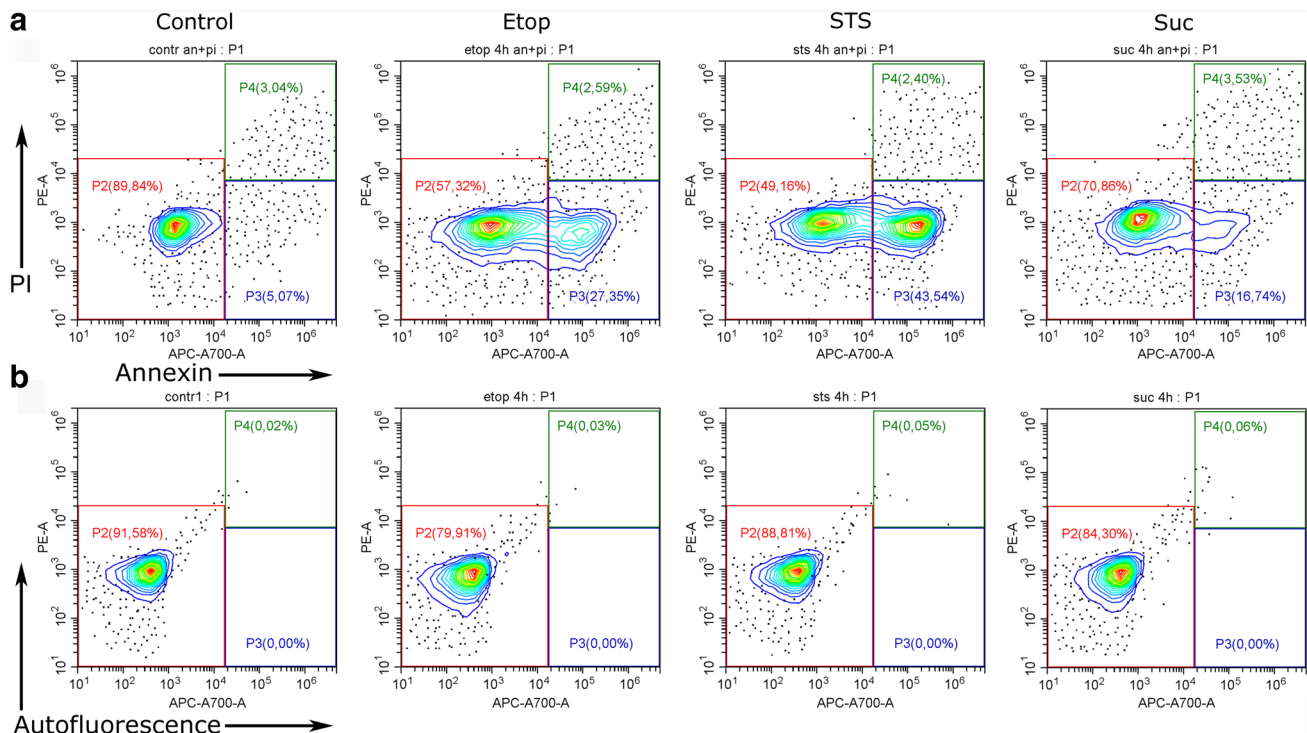


Fig. 3 Normal (P2), early apoptotic (P3) and late apoptotic (P4) subpopulations of U937 cells following 4 h treatment with etoposide, STS and hypertonic sucrose are revealed in annexin versus PI plots. Population percentage indicated next to P2, P3, P4 marks are related to P1 population, i.e. to the non-fragmented cells. The same samples

as in Fig. 1 (a); no subpopulations P3 are observed in unstained cell cultures in the same channels. Residual analog of P2 can be interpreted as autofluorescence (b); a and b data are obtained in one and the same experiment

of particles in the P0 subset increases (compare Figs. 2, 4). The rate of increase in the numbers of early apoptosis cells depends on the inducer (Fig. 4).

Apoptosis progress in cell population P1 as revealed by changes in FSC, SSC, cell size and water content

The CytExpert software gives statistics of particle distribution in individual subsets, in particular, their means and medians. These parameters were used to study fine changes in FSC and SSC during the initial stages of apoptosis, apart from routine counting of particles P0 and P1 separated by crude gating on logarithmic FSC/SSC plots. The initiation of apoptosis with etoposide was found not to be accompanied by any significant increase in the magnitude of the FSC signal for particles in P1 during the first 2 h ($P < 0.01$, Fig. 5). Only later, a decrease in FSC was observed in parallel with an increase in the number of P3 cells, which indicates early apoptosis (Fig. 4). The FSC decrease is frequently interpreted as an evidence of apoptotic shrinkage due to cell water loss. However, in contrast to apoptosis induced in U937 cells by other drugs or apoptosis induced by etoposide in other cell types (e.g. thymocytes), etoposide-induced apoptosis U937 cells does not lead to an

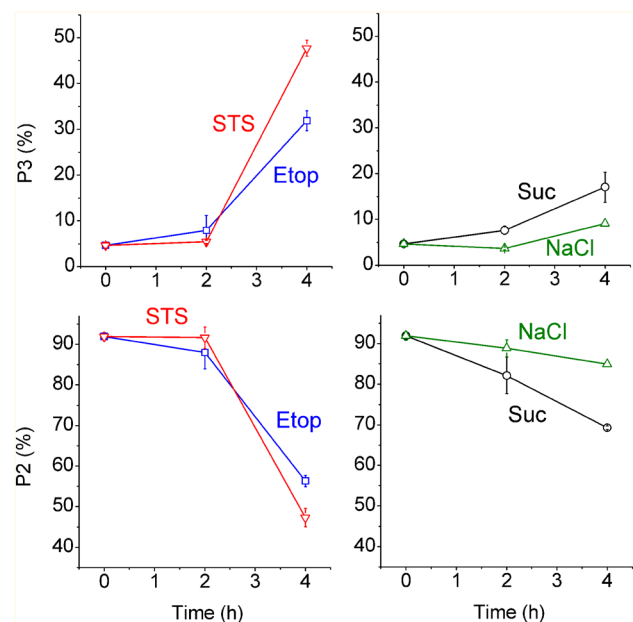


Fig. 4 Time course of an increase in percentage of early apoptotic cell populations P3 and decrease for normal cell populations P2 in cultures treated with etoposide, STS and hypertonic sucrose or NaCl solution. P2 and P3 percentages are calculated for parent population P1. Means \pm SE for 3–4 independent experiments, typical experiment is shown on Figs. 1 and 3

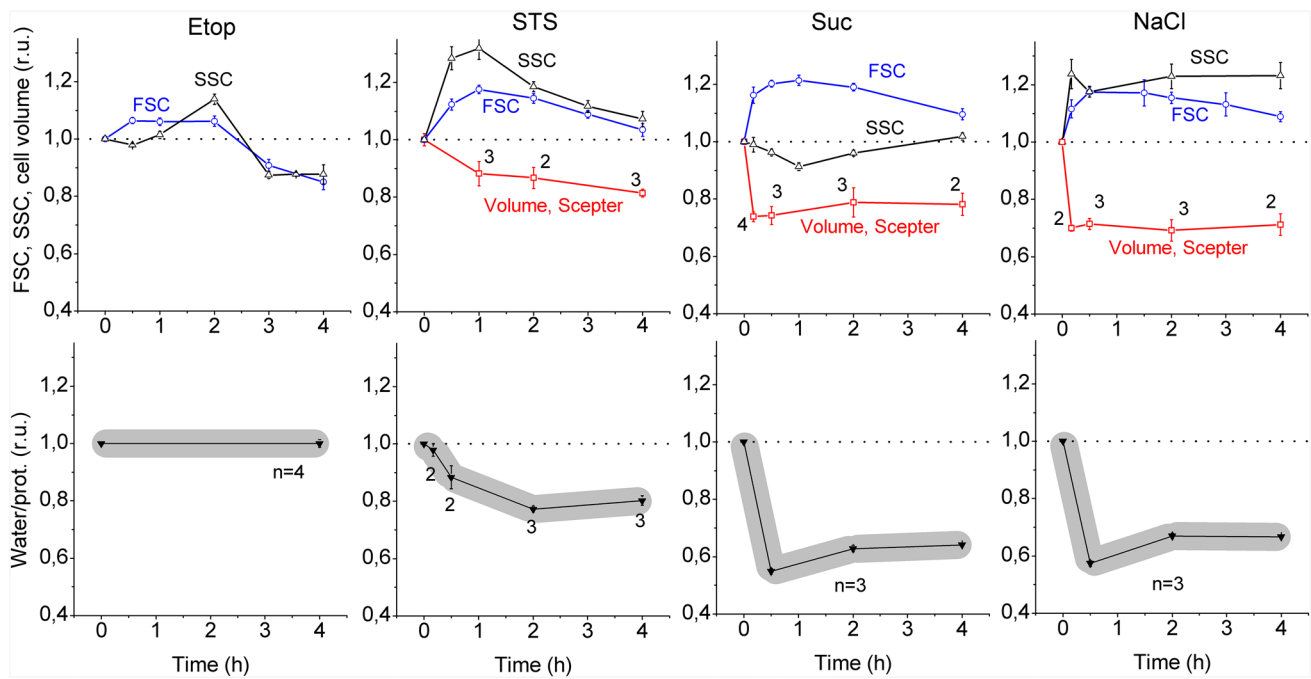


Fig. 5 Time course of changes in FSC, SSC, cell volume and water content of U937 cells induced to apoptosis by etoposide, STS and hypertonic stress as compared with untreated cells of the same batch. Medians by CytExpert software are used to estimate cells P1 FSC and SSC changes and given as means \pm SE for 3–15 experiments. $P < 0.01$ for FSC compared at 0–1 and 2–4 h. Cell volume by Scepter cell

counter is the modes averaged for indicated number of experiments, mean \pm SE. Cell water was estimated by cell buoyant density; *symbols* are means \pm SE, the *gray bands* represent width of cell distribution in density gradient estimated by eye. The number of the experiments for measurement the water/protein ratio is indicated in the graphs

increase in cell buoyant density, i.e. cell dehydration. This was studied in details in our previous work [14] and confirmed in the current experiments (Fig. 5). Figure 6a shows the distribution of U937 cells by electronic size in a sample treated with etoposide for 4 h. There are two distinct subsets in the histogram. One subset may represent cell fragments (P0) and other represents P1 whose average size may be a little smaller than in untreated control.

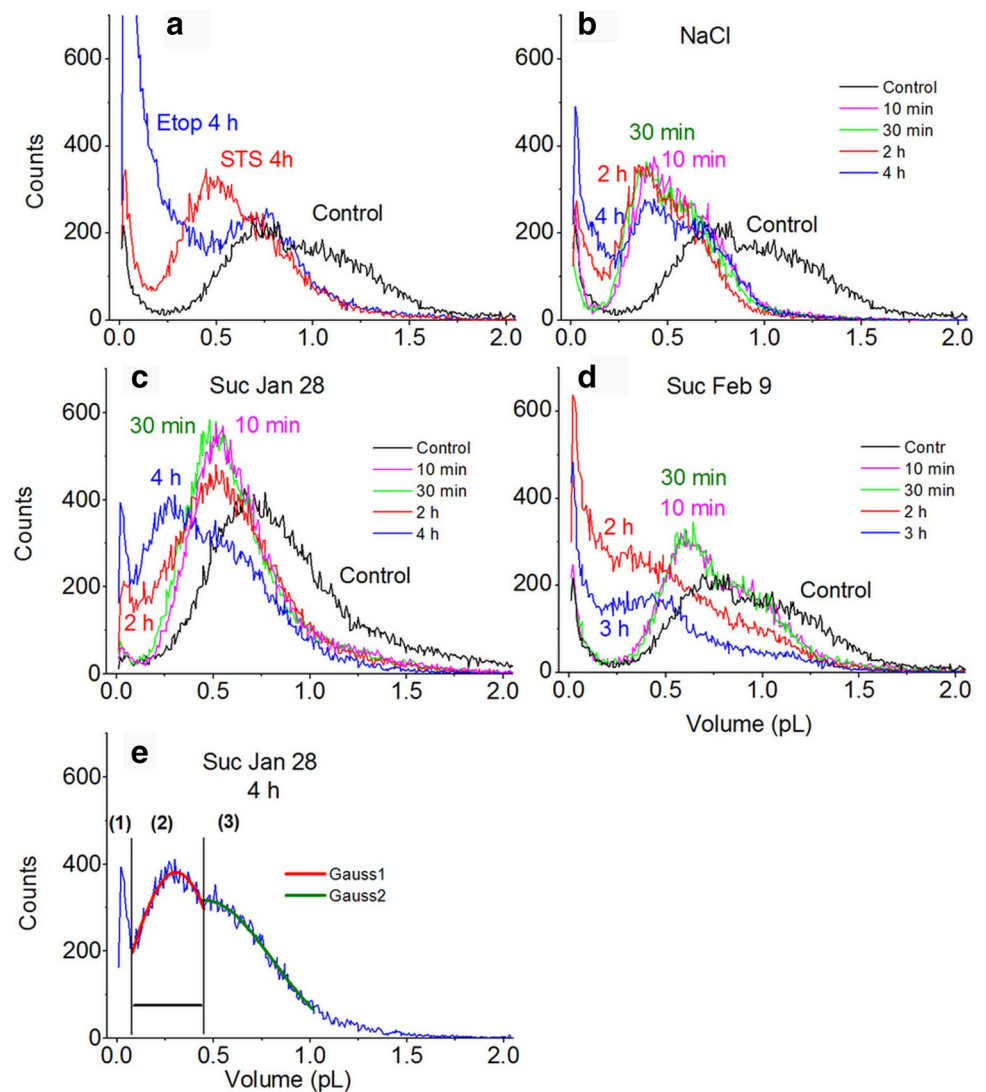
STS-treated cells showed an initial increase in FSC followed by a slow decrease ($P < 0.01$ for comparison 0–1 and 2–4 h, respectively) and, at the same time, the large cell dehydration (Fig. 5). Therefore, the widely shared opinion that a decrease in FSC during apoptosis is a reliable indicator of AVD connected with dehydration appears to be erroneous. The reduced water content of STS-treated cells was shown earlier by cell buoyant density determination [14] and confirmed by the similar assay of the same batch of cells (Fig. 5). The effect of cell dehydration on FSC increase is known [24, 25]. The significant decrease in size of STS treated cells at 4 h is confirmed by determination of cell size by Scepter (Fig. 6a). The FSC level to 4 h is the same as in untreated cells.

The experiment with hypertonic media further supports this explanation: in this case, there is no doubt that shrinkage is caused by the loss of cell water, and yet the FCS

initially increases ($P < 0.01$ for comparison 0–1 h, Fig. 5). The long-term response to hypertonic solution is more complicated. The rapid osmotic dehydration is followed by two opposing processes: a delayed loss of water associated with apoptosis (AVD) and an active response aimed at restoration of the cell volume (regulatory volume increase, or RVI). Apoptosis is also accomplished by formation of diverse microparticles. The corresponding three subsets of cells (microparticles and cells at the AVD and RVI stages) are found on histograms obtained with the Scepter Cell Counter (Fig. 6e). These subsets could not be characterized quantitatively in the histograms but they are still well visible. The data show that, initially, the entire volume distribution shifts to the left (rapid dehydration), but later it begins to split into two: some cells keep shrinking (AVD) and others begin to increase in size (RVI). The numbers of cells experiencing AVD and RVI, as well as the magnitude of volume changes, vary from experiment to experiment (compare Sucrose Jan 28 and Feb 9 in Fig. 6c, d). These two opposite trends, AVD and RVI, have been examined earlier in our publications and by other researchers [3, 16, 20].

Hypertonic stress caused either by 180 mM sucrose or by 100 mM NaCl following a prompt initial FSC increase gives way to a slow FSC decrease similar to that in STS- or

Fig. 6 Cell volume distributions by Scepter Counter in cell cultures induced to apoptosis with etoposide or STS for 4 h (a), and hypertonic NaCl (b), or sucrose solutions (c, d) for indicated time; Gauss approximations assuming three distinct subsets in cells culture treated with sucrose: 1 microparticles of small size, 2 non-fragmented cells with reduced size and 3 non-fragmented cells partly recovering cell volume in direction opposite to AVD (e)



etoposide-induced apoptosis. The FSC at 4 h appears to be about the same as in control. The slow FSC decrease was observed in all studied types of apoptosis. It could be connected with a slow decrease in cell size due to dissociation of apoptotic bodies and with an alteration of cell morphology. Examples of numerous changes in U937 cell morphology during apoptosis caused by hypertonic solutions can be found in our previous publication [20] and those caused by etoposide and STS are shown in Fig. 7. Microscopy also shows a wide variety of microparticles related to the subset P0.

The described changes in FSC characterize the majority of cells in population P1 and apply both to stained and unstained samples. These changes were significant even though the P1 population was heterogeneous: not all cells in P1 have developed annexin staining by 4 h. Apart from the above conclusion a more detailed analysis was

performed. We compared FSC for annexin-positive “early-apoptotic” cells P3 with FSC for annexin-negative “pre-apoptotic” cells P2 in the same samples. In each treatment, annexin-positive cells had a lower FSC signal than cells at a less advanced stage P2. The difference was 20–30% for etoposide and hypertonic apoptosis and only 10% for STS ($P < 0.05$, Fig. 8). Thus, the effect observed for the entire population P1 was confirmed sufficiently well by comparison of the subpopulations P2 and P3.

Discussion

Since the Kerr’s paper [26], cell shrinkage has been accepted as a hallmark of apoptosis. Moreover, there is a concept that cell shrinkage and water loss, i.e. AVD, may trigger the initial stages of apoptosis [1, 3, 27–29].

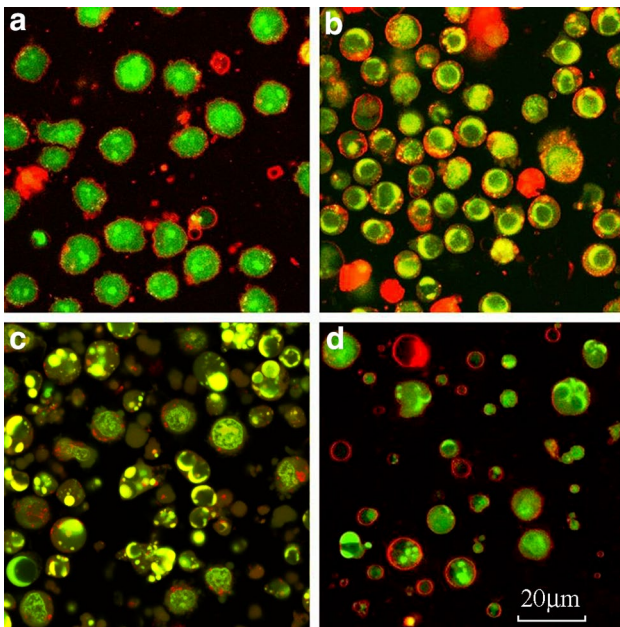


Fig. 7 Confocal images of U937 cells before (a) and after treatment for 4 h with STS (b) or etoposide (c, d). Cells were stained with acridine orange and ethidium bromide; in a combination with RH414 (a, b and d); apoptotic bodies collected from different images (d). Leica TCS-SL microscope was used for confocal microscopy. Other details see in [14]

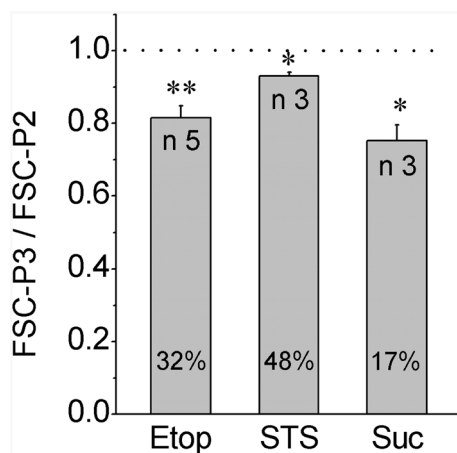


Fig. 8 FSC decrease in early apoptotic cells P3 as compared with cells P2 of the same sample. Cells were treated with indicated apoptosis inducers for 4 h. Mean \pm SE of the ratios FSC-P3/ FSC-P2, number of experiments n and the percentages of P3 cell subpopulation for the used inducers are indicated on the graph. Medians by CytExpert software are used to estimate cells FSC and SSC changes. *, ** $P < 0.05$ and 0.005 respectively as compared to 1 (that corresponds to FSC-P3 = FSC-P2)

Apoptotic cell volume decrease, known as AVD, remains under focus in many studies of apoptosis [6, 10, 11, 30–34]. The most popular way of monitoring AVD is by

flow cytometric light scattering. However, because scattering intensity depends not only on the cell size but also on the extent of cell hydration, which is expected to be affected during early stages of apoptosis, interpretation of the scattering signal as a measure of cell size becomes problematic. Correlation studies of FSC and electronic sizing had been previously done by other authors on human lymphocytes, granulocytes and hamster fibroblasts treated with anisotonic media [24, 25]. It was found, in particular, that a decrease in cell volume in hypertonic media is accompanied by an increase in forward light scattering because the effect of an increase in refractive index (which augments scattering) outweighs the effect of cell size reduction. Detailed studies of electronically measured cell volume on cell fractions sorted by FSC and SSC were performed recently on several cell types and showed that light scattering can be an effective tool for studying cell volume variations, but that depends on the cell type [35, 36]. Parallel studies of changes in light scattering and electronically measured cell size during apoptosis are sparse and controversial [3, 37–40]. A study combining both techniques with determination of cell hydration by the buoyant density assay is performed to our knowledge for the first time.

We conclude that an increase, but not a decrease, in FSC marks the initial cell volume decrease associated with apoptotic dehydration. The delayed FSC decrease occurs along with accumulation of annexin-positive cells. It is similar in apoptosis caused by all of the studied inducers and could be due to dissociation of apoptotic bodies or (and) morphological changes of cells. The popular view that a decrease in FSC reflects the AVD that occurs during initial stages of apoptosis is inconsistent with our data obtained on U937 cells. We suppose that this view gained popularity because cell fragments with reduced sizes have been misinterpreted as dehydrated apoptotic cells. Our initial gating was based on FSC/SSC contour plots, which are more informative than dot plots. Only whole cells identified on FSC/SSC contour plots were analyzed further and tested, in particular, for signs of early apoptosis by annexin and propidium iodide. We believe that initial stages of apoptosis related to cell dehydration should be studied on whole cells to avoid having light scattering affected by cell size reduction due to dissociation of apoptotic bodies. The other advantage of our approach is that fine changes in FSC and SSC were estimated directly by their magnitude provided by the instrument software rather than by simple calculation of the number of cells in each particle subset.

Acknowledgements This study was supported by Russian Foundation for Basic Research, Projects No. 15-04-00776a and No. 17-00-00364 KOMFI.

References

- Maeno E, Ishizaki Y, Kanaseki T, Hazama A, Okada Y (2000) Normotonic cell shrinkage because of disordered volume regulation is an early prerequisite to apoptosis. *Proc Natl Acad Sci U S A* 97:9487–9492. doi:[10.1073/pnas.140216197](https://doi.org/10.1073/pnas.140216197)
- Bortner CD, Cidlowski JA (2011) Life and death of lymphocytes: a volume regulation affair. *Cell Physiol Biochem* 28:1079–1088. doi:[10.1159/000335864](https://doi.org/10.1159/000335864)
- Bortner CD, Scoltock AB, Sifre MI, Cidlowski JA (2012) Osmotic stress resistance imparts acquired anti-apoptotic mechanisms in lymphocytes. *J Biol Chem* 287:6284–6295. doi:[10.1074/jbc.M111.293001](https://doi.org/10.1074/jbc.M111.293001)
- Bortner CD, Cidlowski JA (2014) Ion channels and apoptosis in cancer. *Philos Trans R Soc B* 369:20130104. doi:[10.1098/rstb.2013.0104](https://doi.org/10.1098/rstb.2013.0104)
- Dezaki K, Maeno E, Sato K, Akita T, Okada Y (2012) Early-phase occurrence of K⁺ and Cl⁻ efflux in addition to Ca²⁺ mobilization is a prerequisite to apoptosis in HeLa cells. *Apoptosis* 17:821–831. doi:[10.1007/s10495-012-0716-3](https://doi.org/10.1007/s10495-012-0716-3)
- Lang F, Hoffmann EK (2012) Role of ion transport in control of apoptotic cell death. *Compr Physiol* 2:2037–2061. doi:[10.1002/cphy.c110046](https://doi.org/10.1002/cphy.c110046)
- Wlodkowic D, Telford W, Skommer J, Darzynkiewicz Z (2011) Apoptosis and beyond: cytometry in studies of programmed cell death. *Methods Cell Biol* 103:55–98. doi:[10.1016/B978-0-12-385493-3.00004-8](https://doi.org/10.1016/B978-0-12-385493-3.00004-8)
- Wlodkowic D, Skommer J, Darzynkiewicz Z (2012) Cytometry of apoptosis. Historical perspective and new advances. *Exp Oncol* 34:255–262
- Vanden-Berghe T, Grootjans S, Goossens V, Dondelinger Y, Krysko DV, Takahashi N, Vandenabeele P (2013) Determination of apoptotic and necrotic cell death in vitro and in vivo. *Methods* 61:117–129. doi:[10.1016/j.ymeth.2013.02.011](https://doi.org/10.1016/j.ymeth.2013.02.011)
- Vorobjev IA, Barteneva NS (2015) Temporal heterogeneity metrics in apoptosis induced by anticancer drugs. *J Histochem Cytochem* 63:494–510. doi:[10.1369/0022155415583534](https://doi.org/10.1369/0022155415583534)
- Vorobjev IA, Barteneva NS (2017) Multi-parametric imaging of cell heterogeneity in apoptosis analysis. *Methods* 112:105–123. doi:[10.1016/j.ymeth.2016.07.003](https://doi.org/10.1016/j.ymeth.2016.07.003)
- Banfalvi G (2017) Methods to detect apoptotic cell death. *Apoptosis* 22:306–323. doi:[10.1007/s10495-016-1333-3](https://doi.org/10.1007/s10495-016-1333-3)
- Shapiro HM (2003) *Practical flow cytometry*. 4th edn. Wiley-Liss, New York
- Yurinskaya V, Goryachaya T, Guzhova I, Moshkov A, Rozanov Y, Sakuta G, Shirokova A, Shumilina E, Vassilieva I, Lang F, Vereninov A (2005) Potassium and sodium balance in U937 cells during apoptosis with and without cell shrinkage. *Cell Physiol Biochem* 16:155–162. doi:[10.1159/000089841](https://doi.org/10.1159/000089841)
- Yurinskaya VE, Moshkov AV, Rozanov YM, Shirokova AV, Vassilieva IO, Shumilina EV, Lang F, Volgareva EV, Vereninov AA (2005) Thymocyte K⁺, Na⁺ and water balance during dexamethasone- and etoposide-induced apoptosis. *Cell Physiol Biochem* 16:15–22. doi:[10.1159/000087727](https://doi.org/10.1159/000087727)
- Yurinskaya VE, Rubashkin AA, Shirokova AV, Vereninov AA (2011) Regulatory volume increase (RVI) and apoptotic volume decrease (AVD) in U937 cells in hypertonic medium. *Cell Tissue Biol* 5:487–494. doi:[10.1134/S1990519X11050129](https://doi.org/10.1134/S1990519X11050129)
- Vereninov AA, Rubashkin AA, Goryachaya TS, Moshkov AV, Rozanov YM, Shirokova AV, Strelkova EG, Lang F, Yurinskaya VE (2008) Pump and channel K (Rb⁺) fluxes in apoptosis of human lymphoid cell line U937. *Cell Physiol Biochem* 22:187–194. doi:[10.1159/000149796](https://doi.org/10.1159/000149796)
- Vereninov AA, Volgareva EV, Matveev VV, Moshkov AV, Rozanov I, Shirokova AV, Yurinskaya VE (2003) Water and ion balance in rat thymocytes under apoptosis induced with dexamethasone or etoposide. Iono-osmotic model of cell volume decrease. *Tsitologiya* 45:500–509 (in Russian)
- Vereninov AA, Goryachaya TS, Matveev VV, Moshkov AV, Rozanov YuM, Sakuta GA, Shirokova AV, Yurinskaya VE (2004) Cell shrinkage during apoptosis is not obligatory. Apoptosis of U937 cells induced by staurosporine and etoposide. *Tsitologiya* 46:609–619 (in Russian)
- Yurinskaya VE, Moshkov AV, Wibberley AV, Lang F, Model MA, Vereninov AA (2012) Dual response of human leukemia U937 cells to hypertonic shrinkage: initial regulatory volume increase (RVI) and delayed apoptotic volume decrease (AVD). *Cell Physiol Biochem* 30:964–973. doi:[10.1159/000341473](https://doi.org/10.1159/000341473)
- Yurinskaya VE, Rubashkin AA, Vereninov AA (2011) Balance of unidirectional monovalent ion fluxes in cells undergoing apoptosis: why does Na⁺/K⁺ pump suppression not cause cell swelling? *J Physiol* 589:2197–2211. doi:[10.1113/jphysiol.2011.207571](https://doi.org/10.1113/jphysiol.2011.207571)
- Barteneva NS, Fasler-Kan E, Bernimoulin M, Stern JNH, Ponomarev ED, Duckett L, Vorobjev IA (2013) Circulating microparticles: square the circle. *BMC Cell Biol* 14:23. doi:[10.1186/1471-2121-14-23](https://doi.org/10.1186/1471-2121-14-23)
- Atkin-Smith GK, Tixeira R, Paone S, Mathivanan S, Collins C, Liem M, Goodall KJ, Ravichandran KS, Hulett MD, Poon IKh (2015) A novel mechanism of generating extracellular vesicles during apoptosis via a beads-on-a-string membrane structure. *Nat Commun* 6:7439. doi:[10.1038/ncomms8439](https://doi.org/10.1038/ncomms8439)
- McGann LE, Walterson ML, Hogg LM (1988) Light scattering and cell volumes in osmotically stressed and frozen-thawed cell. *Cytometry* 9:33–38. doi:[10.1002/cyto.990090106](https://doi.org/10.1002/cyto.990090106)
- Sloot PMA, Hoekstra AG, Figdor CG (1988) Osmotic response of lymphocytes measured by means of forward light scattering: theoretical considerations. *Cytometry* 9:636–641. doi:[10.1002/cyto.990090620](https://doi.org/10.1002/cyto.990090620)
- Kerr JF (1971) Shrinkage necrosis: a distinct mode of cellular death. *J Pathol* 105:13–20. doi:[10.1002/path.1711050103](https://doi.org/10.1002/path.1711050103)
- Bortner CD, Cidlowski JA (1996) Absence of volume regulatory mechanisms contributes to the rapid activation of apoptosis in thymocytes. *Am J Physiol* 271:C950–C961
- Maeno E, Takahashi N, Okada Y (2006) Dysfunction of regulatory volume increase is a key component of apoptosis. *FEBS Lett* 580:6513–6517. doi:[10.1016/j.febslet.2006.10.074](https://doi.org/10.1016/j.febslet.2006.10.074)
- Numata T, Sato K, Okada Y, Wehner F (2008) Hypertonicity-induced cation channels rescue cells from staurosporine-elicited apoptosis. *Apoptosis* 13:895–903. doi:[10.1007/s10495-008-0220-y](https://doi.org/10.1007/s10495-008-0220-y)
- Lang F, Hoffmann EK (2013) CrossTalk proposal: cell volume changes are an essential step in the cell death machinery. *J Physiol* 591:6119–6121. doi:[10.1113/jphysiol.2013.258632](https://doi.org/10.1113/jphysiol.2013.258632)
- Orlov SN, Model MA, Grygorczyk R (2013) CrossTalk opposing view: the triggering and progression of the cell death machinery can occur without cell volume perturbations. *J Physiol* 591:6123–6125. doi:[10.1113/jphysiol.2013.258624](https://doi.org/10.1113/jphysiol.2013.258624)
- Kasim NR, Kuželová K, Holoubek A, Model MA (2013) Live fluorescence and transmission-through-dye microscopic study of actinomycin D-induced apoptosis and apoptotic volume decrease. *Apoptosis* 18:521–532. doi:[10.1007/s10495-013-0804-z](https://doi.org/10.1007/s10495-013-0804-z)
- Model MA, Schonbrun E (2013) Optical determination of intracellular water in apoptotic cells. *J Physiol* 591:5843–5849. doi:[10.1113/jphysiol.2013.263228](https://doi.org/10.1113/jphysiol.2013.263228)
- Model MA (2014) Possible causes of apoptotic volume decrease: an attempt at quantitative review. *Am J Physiol Cell Physiol* 306:C417–C424. doi:[10.1152/ajpcell.00328.2013](https://doi.org/10.1152/ajpcell.00328.2013)
- Tzur A, Moore JK, Jorgensen P, Shapiro HM, Kirschner MW (2011) Optimizing optical flow cytometry for cell volume-based

- sorting and analysis. PLoS ONE 6(1):e16053. doi:[10.1371/journal.pone.0016053](https://doi.org/10.1371/journal.pone.0016053)
36. Vecsler M, Lazar I, Tzur A (2013) Using standard optical flow cytometry for synchronizing proliferating cells in the G1 phase. PLoS ONE 8:e83935. doi:[10.1371/journal.pone.0083935](https://doi.org/10.1371/journal.pone.0083935)
37. Ormerod MG, Paul F, Cheetham M, Sun X-M (1995) Discrimination of apoptotic thymocytes by forward light scatter. Cytometry 21:300–304. doi:[10.1002/cyto.990210311](https://doi.org/10.1002/cyto.990210311)
38. Bortner CD, Sifre MI, Cidlowski JA (2008) Cationic gradient reversal and cytoskeleton-independent volume regulatory pathways define an early stage of apoptosis. J Biol Chem 283:7219–7229. doi:[10.1074/jbc.M707809200](https://doi.org/10.1074/jbc.M707809200)
39. Franco R, DeHaven WI, Sifre MI, Bortner CD, Cidlowski JA (2008) Glutathione depletion and disruption of intracellular ionic homeostasis regulate lymphoid cell apoptosis. J Biol Chem 283:36071–36087. doi:[10.1074/jbc.M807061200](https://doi.org/10.1074/jbc.M807061200)
40. Mulvey CS, Zhang K, Liu WB, Waxman DJ, Bigio IJ (2011) Wavelength-dependent backscattering measurements for quantitative monitoring of apoptosis, Part 2: early spectral changes during apoptosis are linked to apoptotic volume decrease. J Biomed Opt 16:117002. doi:[10.1117/1.3644911](https://doi.org/10.1117/1.3644911)